



Contents lists available at ScienceDirect

Innovative Food Science and Emerging Technologies

journal homepage: www.elsevier.com/locate/ifset

On-line and non-destructive measurement of core temperature in heat treated fish cakes by NIR hyperspectral imaging

Jens Petter Wold *

Nofima, Norwegian Institute for Food and Fisheries Research, Muninbakken 9-13, Breivika, NO-9291 Tromsø, Norway

ARTICLE INFO

Article history:

Received 10 September 2015

Accepted 10 December 2015

Available online xxxx

Keywords:

Core temperature

On-line NIR

Hyperspectral imaging

Industrial heat treatment

Food safety

ABSTRACT

During industrial heat treatment of food products the core temperature is a critical control parameter with respect to food quality and in particular food safety. This paper presents a method based on near-infrared (NIR) spectroscopy that enables on-line and non-contact monitoring of the complete product volume on a typical industrial belt cooking system. Two NIR systems (760–1040 nm) were evaluated on heat treated fish cakes, one point measurement system and one hyperspectral imaging system. Both systems measured several millimetres into the product. Core temperature in the fish cakes (at 10 mm depth) varied between 53 and 99 °C. The point system performed best with a root mean square error of prediction of 2.3 °C, while the imaging system was less accurate with an error of 4.5 °C. It was demonstrated that temperature changes down to 11–13 mm depth in the fish cakes could be registered by the NIR point system.

Industrial relevance: During industrial heat treatment of food products the core temperature is a critical control parameter with respect to food quality and in particular food safety. Especially for ready-made products this is important since they can be consumed without further heat treatment. Today, most temperature measurements during processing are typically based on spot checks on a small number of products. The core temperature of heat treated products is usually the most critical and needs to be measured by insertion of thermo couplers. This procedure is insufficient since it leaves the producer with a large degree of uncertainty; only a few products are checked and a very tiny volume of the checked products is actually measured. Due to these limitations, current practise is to over-cook much of the food to ensure that everything has reached the critical core temperature. This might reduce quality of the end product and also requires overspending of energy. In the food industry there is a need for non-contact on-line temperature measurements for improved control of the cooking process. The ideal system should be able to log the temperature in the entire production volume.

The method presented in this article can allow complete monitoring of the heat treated products. In this way the producer could have full control of the heating process and be sure that sufficient core temperature is reached in all product units. Such a system can also be used to control the temperature to a certain target that ensures safe products of high quality.

© 2015 Elsevier Ltd. All rights reserved.

1. Introduction

During industrial heat treatment of food products the core temperature is a critical control parameter with respect to food quality and in particular food safety. Especially for ready-made products this is important since they can be consumed without further heat treatment. Today, most temperature measurements during processing are typically based on spot checks on a small number of products. The core temperature of heat treated products is usually the most critical and needs to be measured by insertion of thermo couplers. This procedure is insufficient since it leaves the producer with a large degree of uncertainty; only a few products are checked and a very tiny volume of the checked

products is actually measured. Due to these limitations, current practise is to over-cook much of the food to ensure that everything has reached the critical core temperature. This might reduce quality of the end product and also requires overspending of energy. In the food industry there is a need for non-contact on-line temperature measurements for improved control of the cooking process. The ideal system should be able to log the temperature in the entire production volume.

There are non-contact temperature measurement in use today based on IR measurements and imaging, but these instruments probe the surface of the products and not the inner part (Gowen, Tiwari, Cullen, McDonnell, & O'Donnell, 2010). When the heating process is well defined it is possible to estimate the core temperature in e.g. cooked chicken breast by combining non-contact surface temperature with process information like time of heating, heating temperature, etc. (Ibarra, Tao, & Xin, 2000). This approach requires detailed quantitative knowledge of the process and how it affects the temperature in the

* Corresponding author at: Nofima AS, Osloveien 1, 1430 Ås. Tel.: +47 95979749; fax: +47 64970333.

E-mail address: jens.petter.wold@nofima.no.

products. It would be better to be able to measure the actual core temperature directly.

Near-infrared spectroscopy is widely used for rapid determination of food composition. The method is recognised for its rapidity, robustness and versatility with regard to sampling. It is possible to sample rather large surfaces and volumes, the NIR radiation can penetrate relatively deep into bio-materials, and the measurement principle lends itself well to hyperspectral imaging at a macroscopic level. Applications of NIR imaging are already established in the food processing industry for e.g. quality grading of crabs, salmon fillets and pork meat (Wold et al., 2006; Segtnan, Høy, Lundby, Narum, & Wold, 2009; O'Farrell et al., 2010), and the opportunities are versatile. It is well known that the near-infrared spectrum of water is affected by sample temperature (Buning-Pfaue, 2007). The absorption bands of water are shifted to longer wavelengths with decreasing temperature. The water has absorption peaks at 840 nm, 970 nm, 1190 nm, 1450 nm, and 1940 nm due to a combination of different overtones of OH stretching and bending bands. This temperature shift complicates calibration models based on NIR for samples with varying temperature, since this effect has to be accounted for (Chen & Martin, 2007). On the other hand, the phenomenon can also be used to monitor the temperature in materials. Monitoring of tissue temperature has been reported for medical purposes by Chung, Cerussi, Merritt, Ruth, and Tromberg (2010) who used NIR spectroscopy around 990 nm to measure temperature in model samples as well as in human underarms. Hollis, Binzoni, and Delpy (2001) proposed NIR as a non-invasive method for brain tissue temperature during surgery. Based on simulations they suggested that it would be possible to detect changes in temperature down to about 15 mm depth by using the wavelength range 700–1000 nm. This can be done by illuminating the brain at one spot and detecting the light a distance away to ensure that the light travels to certain depths, a measurement mode termed *interactance*. The same approach has been used to measure core temperature in baked liver pate (O'Farrell et al., 2011). They used an NIR instrument that was originally designed to measure fat content in live salmon; high power NIR radiation is transmitted through the skin of the fish, and detection of the returning light in the range 760–1040 nm is used to estimate the fat content in the fish muscle (Folkestad et al., 2008). The same deep penetrating system has been used to measure dry matter content in whole potatoes with skin (Helgerud et al., 2015). Quite good results were obtained for temperature monitoring in liver pate, with prediction errors in the range 1.5–4.3 °C. A challenge when measuring core temperature in materials like liver pate or brain is that the measured NIR signal is affected not only by the core temperature, but also the temperature gradient from surface and down toward the core. O'Farrell et al. (2011) demonstrated that large prediction errors could occur for test samples with temperature gradients different from the calibration set.

Rapid and non-destructive quantification and imaging of ice fraction in super chilled salmon fillets is another interesting and relevant application reported by Ottestad, Høy, Stevik, and Wold (2009). This was done on-line with NIR in interactance mode utilising the very large shift in the water absorption peak that occurs when water turns into ice. The system produced images of salmon fillets with a quantitative distribution of ice fraction within each fillet.

The objective of this paper was to evaluate the feasibility of measuring core temperature in heat treated fish cakes on-line and non-contact by NIR spectroscopy. The fish cakes had a large variation in both core temperature and temperature gradients. Two different instruments were tested and compared: an NIR interactance system with a rather deep optical penetration, the same as used by O'Farrell et al., (2011), but in this study the measurements were done without contact between sample and instrument. The other system used was a commercial on-line hyperspectral NIR imaging scanner, the same as the one used by Ottestad et al. (2009). This scanner has a penetration depth of approximately 10 mm and it can measure samples across the whole width of a typical conveyor belt and could give the opportunity to monitor the

temperature in all products after heat treatment in a typical industrial band-cooker. A sampling experiment was also conducted to estimate how deep into the samples temperature was measured.

2. Materials and methods

2.1. NIR spectroscopy

The point NIR system was originally designed to measure fat and pigment in the muscle of live salmon (Folkestad et al., 2008). Two halogen light sources of 50 W each illuminate the sample in two rectangular regions of 5 mm * 20 mm size. Distance between the two illuminated regions is 10 mm. The system collects the light that has penetrated down into the sample and comes up again in a small area of 4 * 4 mm between the two illuminated rectangles. The collected light has travelled from an approximate circular area of typically $D = 3$ cm and from depths down to 1–2 cm, depending on the material. The mode of measurement is called interactance and makes it possible to measure through the skin of a salmon to sample the muscle below. It is also possible to measure rather deep down into a fish cake to probe for the core temperature. The system measures at 15 wavelengths in the region 760–1040 nm, spectral bandwidth is 20 nm. The system hardware is calibrated by using a white reference, a barium sulphate through with a curved base. It is held under the instrument allowing the light to pass from the field of illumination to the field of view. The system does about 70 measurements per second and these were averaged over the total measurement time of 1 s per sample. The system is also described in O'Farrell et al. (2011).

The other system was a commercial on-line NIR imaging scanner (QMonitor, TOMRA AS, Asker, Norway). It has been described in detail in several scientific articles concerning on-line quality determination of foods (Wold et al., 2006; ElMasry & Wold, 2008; Wold, Kermit, & Woll, 2010). The scanner was installed above a conveyor belt suitable for foods. The belt was black to reduce stray light. The NIR instrument is based on interactance measurements where the light was transmitted into the fish cake and then back scattered to the surface. The exact optical sampling depth of the cakes was not known, but approximately 10 mm was assumed. The scanner was placed 12 cm above the conveyor belt and the illuminating field was focused on to the belt in a line perpendicular to the direction of movement. The field of spectral collection was parallel to the illuminating field approximately 1 cm further down the conveyor. It was focused on the detector using a cylindrical lens. A blackened metal shield blocked the light between the field of illumination and the field of detection. This ensured that the system mainly measured the light which had traversed the interior of the fish cake and not the direct reflected light from the surface.

The light source consisted of 8 halogen lamps of 50 W each. The scanner collected spectral images of 15 wavelengths between 760 and 1040 nm with a spectral resolution of 20 nm, the same as the non-imaging system described above. The output was an image of the conveyor belt with samples. Size of the image was 64 pixels in the direction perpendicular to belt movement and typically 200 pixels for single fish cakes in the direction of belt movement. It typically took 0.5 s to scan one fish cake.

2.2. Materials

Two batches of fish cake batter were made based on the same formula: fillet of haddock (30 kg), spice mix (2.0 kg), salt (0.70 kg), potato flour (3.8 kg), whole milk (30 kg), and soy oil (1.5 kg).

2.3. Heat treatment and measurements

Cakes were made of the batter and heat treated on a large baking-plate, 9 cakes at the time. They were about 2 cm thick and 10 cm in diameter. They were all fried for 4 min on the first side before they were

turned around. After turning around, the first cake was measured after 2 min and then they were measured successively with about 1 min separation in time. That is, the cakes were measured approximately after 2, 3, 4, 5, 6, 7, 8, 9 and 10 min baking on the other side. This resulted in cakes with large difference in core temperature. The temperature gradients in the cakes would also differ notably with time of baking.

After baking, each cake was placed on a black plastic plate and was immediately (within 3 s) measured under the NIR point system. The measurement was done on the middle of the cake. Measurement time was 1 s. The measurement was without contact, approximately 1 cm separated the cake and the NIR system.

Immediately after this measurement, the temperature was measured with a sensitive and rapid response insertion thermocouple. Temperature was logged at the centre of the fish cake at three depths; 0.5 cm, 1 cm (core) and 1.5 cm. The temperature loggings were done by the same person all the time to avoid differences in measurement procedure.

Then the cake was sent on a conveyor belt for on-line scanning by the NIR imaging scanner. The scanning of each cake took maximum 0.5 s. The whole measurement procedure, including all measurements, was performed within approximately 25 s after the cake left the baking-plate.

These measurements were done for two batches of fish batter, one batch resulted in 64 cakes, and the other in 63 cakes. From the last batch there were also made up a set of 9 fish cakes with varying temperatures. They were placed on the conveyor belt in a 3 * 3 square orientation and scanned by the NIR system for visualisation. Core temperature was measured in all 9 cakes before scanning.

2.4. Depth of measurement

An experiment was conducted on ready-made fish cakes to investigate how differences in temperature at different depths affected the temperature estimated by NIR. This was done by insertion of thin layers (about 2 mm thick) of fish cake holding 20 °C at different depths, in a fish cake holding about 65 °C (Fig. 1). The fish cakes were prepared in advance; a 2 mm layer of the fish cake was cut out by knife. This was done for ten fish cakes, and the layers were cut out at different depths, from the top layer (0 mm) down to about 16 mm. The thin layers were packed and sealed in plastic bags and placed in a water bath of 20 °C. The rest of the fish cakes were sealed in separate bags and put in a water bath of 70 °C. The samples were kept in the water bath for about 45 min before measurements. One fish cake was taken up from the warm water and the matching slice was taken from the 20 °C water. The core temperature of the warm cake without the slice was immediately measured with a thermo coupler (within 10 s of retrieval from water), it was then measured twice by the NIR point system at two different spots. Then the 20 °C slice was put in between (or on top of) the warm parts of

the cake. The two NIR measurements were repeated. In this way we obtained NIR measurements on fish cakes with and without a defined colder layer at different depths.

In connection with this experiment, measurements were collected for a dedicated NIR calibration for temperature in ready-made fish cakes heated in water bath. The fish cakes used in the calibration were heated in a water bath gradually from 40 °C to 80 °C. They were packed in plastic bags in the same way as described above. They were taken up from the water one and one as the water got warmer. Each cake was measured once; first core temperature with a thermo coupler, and then immediately an NIR measurement. A total of 36 cakes were measured and core temperature varied from 35 °C to 76 °C. It was noticed that the there was very little temperature variation as function of depth in these cakes, the water bath heating resulted in homogeneous temperature distribution.

The obtained calibration for temperature was applied on the NIR measurements on fish cakes with and without the cold layer. In that way it was possible to measure the effect the cold layer at different depths had on the estimated temperature of the fish cake. Two estimated temperatures were obtained from each state and one-way ANOVA was used to calculate whether the differences in temperature at different depths were significant or not.

2.5. Spectral preprocessing and calibration

Spectra from the imaging scanner were automatically extracted by the use of a Matlab script. The script imports the hyperspectral image into Matlab and detects the fish cake based on a threshold criterion. The centre of the round fish cake was localised and a rectangular pixel region of interest (ROI) was defined, which covered an area of about 3 cm * 3 cm on the middle of the cake. This ROI consisted of typically 120 pixels. The raw spectra from these pixels were averaged to make one mean spectrum from each fish cake. From here the spectral preprocessing was done in the same way for the two instruments.

The spectra were linearised using the logarithm of the inverse of the interactance spectrum $\log_{10}(1/T)$. To reduce light scattering effects the $\log_{10}(1/T)$ spectra were normalised by standard normal variate (SNV) (Barnes et al., 1989). That is, for each spectrum the mean value was subtracted and the spectrum was then divided by the standard deviation of the spectrum.

Calibration models were made by partial least squares regression (Martens & Næs, 1993). Calibration models were made based on fish cakes from one batch of batter ($n = 64$) and the models were tested on the fish cakes from the other batch of batter ($n = 63$). Performance of the models was estimated by squared correlation (R^2) between measured and estimated temperature, and the root mean square error of prediction (RMSEP) defined as

$$RMSEP = \sqrt{\frac{1}{N} \sum_{i=1}^N (y_i - \hat{y}_i)^2}$$

where \hat{y}_i is the predicted value, y_i is the measured reference value and i denotes the samples from 1 to N . Root mean square error of cross validation (RMSECV) was used to determine the optimal number of components to include in the calibration models.

The regression vector for the calibration based on the imaging system was applied pixel wise in the hyperspectral images resulting in images of the core temperature distribution. These were compared to reference measurements of temperature.

Multivariate calibrations were made by use of the software The Unscrambler version 9.8 (CAMO Software AS, Oslo, Norway) while image processing and spectral pre-treatment were performed in Matlab version R2007b (The Mathworks Inc., Natic, MA).

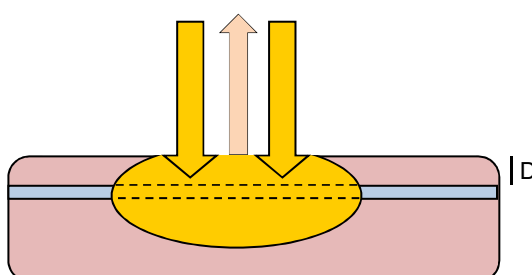


Fig. 1. Sketch of optical measurement with cold layer inserted in warmer fish cake. The two yellow arrows indicate incident light, the pink arrow indicates light from the interior of the cake measured by the detector. D indicates the depth of cold layer in fish cake.

3. Results and discussion

3.1. Temperature measurements

Temperature in the fried fish cakes varied according to Table 1. Calibration and test set covered more or less the same temperature range. Since the cakes were fried on a conventional pan, first on one side and then on the other side, there were clear temperature gradients in the cakes, which varied with baking time. Fig. 2 shows how temperature typically varied in the cakes during baking time from 5 to 13 min, that is, from 1 to 9 min after the cake was turned around in the pan. Measurements at each time represent different cakes, so the figure does not show the development for one cake. In the beginning, the lowest temperature was at 15 mm depth, since this was close to the upper surface during the first 4 min. During the second baking period this part was closest to the pan, and the temperature here increased and exceeded the core temperature and the temperature at 5 mm depth. The core temperature was not necessarily the lowest, as it often will be in industrial baking processes where the products are baked from both sides at the same time. Temperature at 5 mm depth tended to be lowest at the end of the baking time. It is important to note that there were clear temperature gradients in the cakes, and that they varied in direction; increasing temperature from top surface and down in the cake early in the process, and decreasing at the end of the process. This made the samples rather complex and heterogeneous from an optical measurement point of view.

3.2. Spectral measurements

Fig. 3 shows normalised (SNV) spectra from the same samples with the point NIR system and the imaging scanner. The shapes of the spectra are slightly different, however, the main features are the same. The water absorption peak at around 970 nm originating from the second overtone of the OH stretching bond dominates the spectra. A smaller water peak can be seen at 840 nm (combination of the third overtone OH stretching and OH bending bands). Water also has a broad absorption band peaking at about 740 nm, which will affect our spectra in the lower wavelengths (760–780 nm). All these three absorption bands are affected by temperature and shifts and intensity variation will occur (Hollis et al., 2001). Shifts are most easily seen in the 970 nm peak, which is shifted towards shorter wavelengths with increasing temperature. Similar systematic changes in the less intense absorption bands at 760 nm and 840 nm are difficult to discern, however, the effect is reported (Hollis, 2001). An important aim with these NIR measurements was to penetrate deep enough to measure the core temperature. The bands at 760 nm and 840 nm might then be of particular interest, since these wavelengths are less absorbed by water compared to radiation at 970 nm, and therefore have the potential to penetrate deeper into the tissue. For measurements with the point NIR system these wavelengths were absorbed about ten times less than those around 970 nm.

3.3. Calibration results

Table 2 shows the results for both calibration set and test set for the NIR point system. The correlations and prediction error estimates for the calibration set were obtained by cross validation. It can be seen that SNV corrected spectra tend to give more accurate models than non-treated absorption spectra. This was as expected, since we are

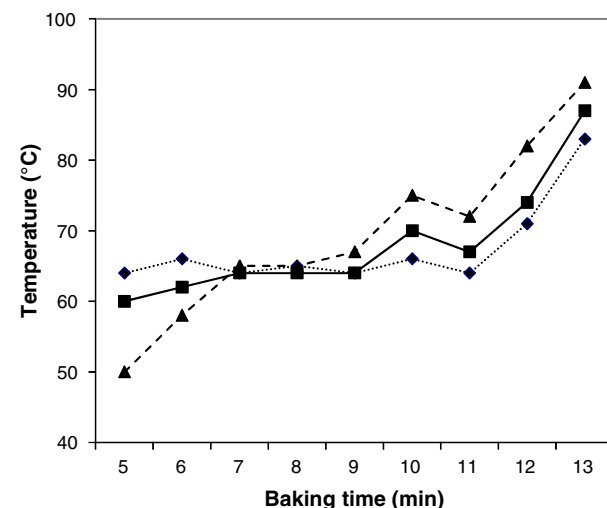


Fig. 2. Typical temperature distribution at 0.5 cm (dotted line), 1 cm (solid line) and 1.5 cm (dashed line) depth in fish cakes as function of baking time.

mainly modelling on spectral shifts. Large offset variations within the absorption spectra did not contribute to explain variation in temperature. These offsets are removed with SNV. The calibration model for raw absorption spectra applied on temperature at 0.5 cm depth consists of 3 PLS factors and gives a notably lower correlation than the SNV corrected spectra. This is probably because the subtle shift information is buried in large offset variations and is difficult to extract.

For models based on SNV corrected spectra, it is clear that the best models were obtained for temperatures at 0.5 cm and about 1 cm (in the core). For temperature at 1.5 cm depth, the accuracy of the models was considerably less, most likely because the system did not probe this deep.

In a comparable study on NIR to model temperature in heat treated liver pate (O'Farrell et al., 2011) similar prediction errors were obtained as long as the temperature regime of baking was the same. In their work, only 2–3 PLS factors were required to establish good calibration models. The reason for the more complex models in this case, requiring as many as 7–9 PLS factors, was probably due to more variation in temperature gradients in the fish cakes. As pointed out above, in some cakes there were no gradients, in others the temperature decreased or increased from surface and down into the cake. Another aspect is that the protein in the cakes would be denatured to a varying extent, which can affect light scattering properties as well as absorption properties. A large number of factors in the calibration model increase the chance of overfitting. However, the models worked well on the test set, and comparable correlations and prediction errors as with the calibration models were obtained.

As also pointed out by O'Farrell et al. (2011), temperature gradients in the heat treated products will affect the prediction results, and it is therefore important that the calibrations are based on the expected process variation.

Hollis et al. (2001) made NIR based calibration models for temperature in pure water and obtained a standard error of prediction (SEP) of about 0.1 °C. When applying the same method on a human underarm, the SEP increased to about 1.1 °C. Absorption and light scattering properties in tissues are much more complex and result in lower accuracy, as with the fish cakes in this study.

As mentioned above, it is of interest to know what part of the spectrum that contributes to explain variation in temperature. Calibration models were therefore made based on the short wavelength range 760–900 nm, including the 840 nm water peak and the tail of the peak at 740 nm, and the long wavelength range, 900–1040 nm, including the peak at 970 nm. The short wavelength range gave best models with prediction error (RMSEP) below 3 °C, while the long range got

Table 1

Overview of logged temperatures in fish cakes. Temperatures are given in °C.

Data set	5 mm	Core (10 mm)	15 mm
Calibration (<i>n</i> = 64)	49–98	53–99	50–99
Test set (<i>n</i> = 63)	51–97	54–98	46–99

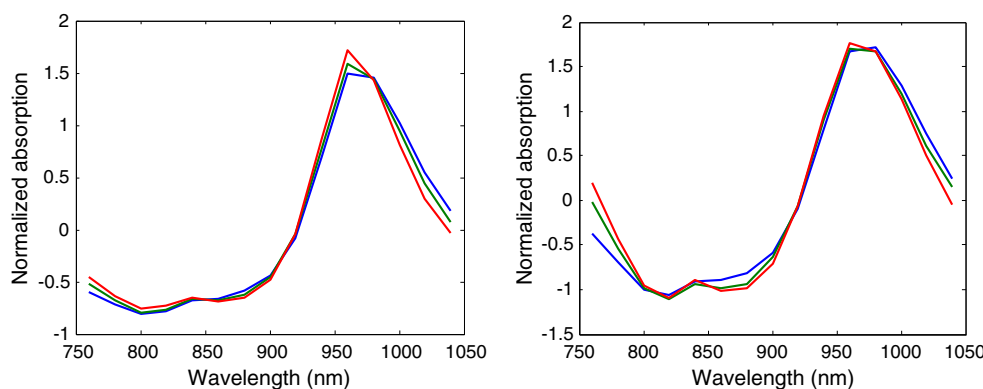


Fig. 3. Normalised NIR spectra from NIR point system (left) and NIR hyperspectral imaging scanner (right). Core temperatures of fish cakes were 51 °C (blue line), 72 °C (green) and 92 °C (red).

RMSEP values just above 4 °C. This indicates that the short wavelength range carries more information than the long range, but the whole range gave the best performance.

The imaging scanner data gave overall less accurate models compared to the point system (Table 3). Four PLS factors were required for all models independent of spectral pre-processing. Difference in results between raw absorption spectra and SNV corrected were small. The main reason for the difference in performance between the two systems is probably the better signal to noise ratio in the point system and that it measured deeper into the fish cakes. The optics was designed to measure deep into tissue and at the same time obtain spectra with as little noise as possible. The scanner uses in principal the same optical measurement mode but was not optimised the same way. With more noise in the spectra, it is less systematic spectral variation to model.

There was a tendency that spectra extracted from the centre of the fish cakes gave slightly better models than average spectra from the whole cake. This can be due to varying temperatures across the cakes, so that the most accurate models are obtained for pixel spectra extracted from the area where the temperature was measured. This was supported by making models for ROIs toward the edges of the cakes. We then obtained even less accurate models, apparently because there was a mismatch between area of optical sampling and temperature sampling. For SNV corrected spectra the RMSEP for calibration and test set increased to 4.5 °C and 5.4 °C for 0.5 cm and 1.0 cm depth, respectively. Prediction performance for the two systems are shown in Fig. 4.

The temperature variation across fish cakes can be visualised in the prediction images of temperature (Fig. 5). Although the image resolution from the NIR scanner is low, it is easy to distinguish single fish

Table 2
Calibration and test results for core temperature in fish cakes based on point NIR.

Calibration (n = 64)									
Spectra	0.5 cm			1.0 cm (core)			1.5 cm		
	No. factors	R ²	RMSEC	No. factors	R ²	RMSEC	No. factors	R ²	RMSEC
Abs	3	0.91	3.10	8	0.95	2.63	9	0.87	4.61
SNV	7	0.96	2.13	8	0.97	2.16	8	0.89	4.34
Test (n = 63)									
Spectra	No. factors			R ²			RMSEP		
	No. factors	R ²	RMSEP	No. factors	R ²	RMSEP	No. factors	R ²	RMSEP
Abs	3	0.88	4.22	8	0.94	2.49	9	0.88	4.28
SNV	7	0.95	1.98	8	0.95	2.34	9	0.86	4.70

RMSEC/P – root mean square error of cross validation/prediction.

R² – squared correlation coefficient.

No. factors – number of factors in the PLS regression model.

Abs – absorption spectra.

SNV – normalised absorption spectra.

cakes. Some cakes are connected in the image because they were close to each other on the belt. In the image there is a large variation in temperature between the cakes, and from the colour scale it can be seen that the estimated temperatures at pixel level corresponded quite well with the measured values.

3.4. Depth of measurement

The calibration model for temperature based on the 36 cakes heated in water bath required only 3 PLS components and had an R² of 0.986 and RMSECV of 2.0 °C. The much simpler model with few components was due to the homogeneous temperature distribution in these cakes. This model was more similar to the models reported by O'Farrell et al., (2011) and also the shape of the regression vector was similar to those of temperature in liver pate (not shown).

The differences in estimated temperature between cakes without and with a cold layer were significant to a depth of 11 mm, that is, the cold layer was positioned from about 11–13 mm depth (Fig. 6). At

Table 3

Calibration and test results for core temperature in fish cakes based on NIR imaging scanner.

Calibration (n = 64)									
Spectra	0.5 cm			1.0 cm (core)			1.5 cm		
	No. factors	R ²	RMSEC	No. factors	R ²	RMSEC	No. factors	R ²	RMSEC
Abs avg	4	0.85	4.00	4	0.81	5.26	4	0.68	7.40
Abs cent	4	0.89	3.50	4	0.84	4.77	4	0.70	7.17
SNV avg	4	0.88	3.68	4	0.84	4.88	4	0.75	6.49
SNV cent	4	0.88	3.56	4	0.85	4.65	4	0.72	6.91
Test (n = 63)									
Spectra	No. factors			R ²			RMSEP		
	No. factors	R ²	RMSEP	No. factors	R ²	RMSEP	No. factors	R ²	RMSEP
Abs avg	4	0.84	3.72	4	0.79	4.96	4	0.68	6.95
Abs cent	4	0.86	3.58	4	0.83	4.53	4	0.70	6.71
SNV avg	4	0.86	3.56	4	0.81	4.78	4	0.73	6.31
SNV cent	4	0.88	3.29	4	0.83	4.53	4	0.74	6.24

RMSEC/P – root mean square error of cross validation/prediction.

R² – squared correlation coefficient.

No. factors – number of factors in the PLS regression model.

Abs – absorption spectra.

SNV – normalised absorption spectra.

avg – average spectrum from whole fish cake.

cent – average spectrum from centre of fish cake.

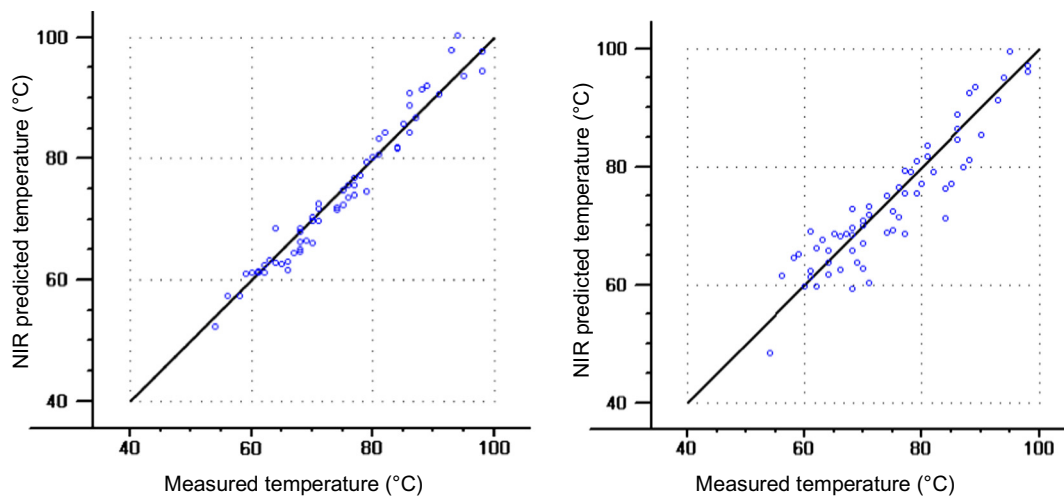


Fig. 4. Predicted versus measured core temperature in test set of fish cakes measured by NIR point system (left) and NIR hyperspectral scanner (right).

greater depths, no significant differences were found. The result indicates that temperature changes at 11–13 mm depth will affect the optical readings and consequently the output of calibration models. The largest differences were found in the upper 7 mm layer, so we can assume that the main contribution to the measured NIR spectrum comes from this layer. The optical signals from the core (at about 10 mm depth) contribute little to the measured signal compared to the upper layers. This stresses that the temperatures in upper layers must correlate with the core temperature in some way, and that it is important that possible temperature gradients are accounted for and included in the calibration models. The result also illustrates an important reason for why calibration models for temperature at 15 mm depth did not perform well.

The result from the experiment gives a good overall approximation of depth sampling, but it should be noted that there were some uncertainty factors. The 2 mm thick slices could vary slightly in thickness since it was difficult to cut them precise. It could also be difficult to obtain the exact depth across the whole cake.

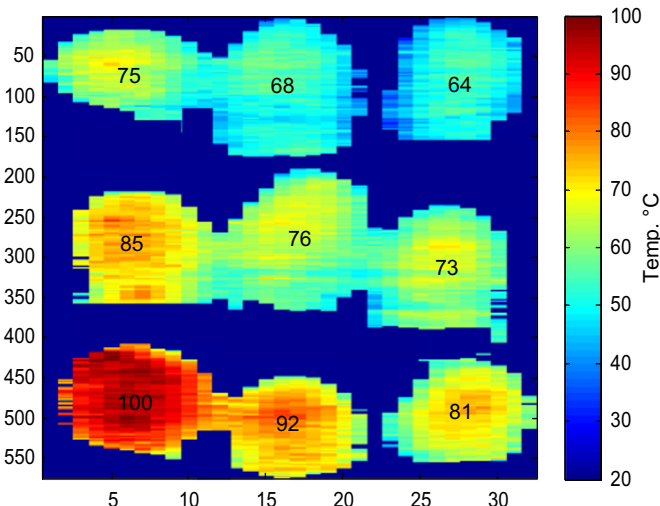


Fig. 5. Prediction image of core temperature in 9 fish cakes based on NIR imaging scanner. Numbers at the centre of the cakes indicate core temperature measured with thermocoupler.

4. General discussion

The results show that NIR interactance is a feasible way to measure and estimate core temperature in fish cakes in a rapid and non-destructive way with no physical contact with the instrument. The NIR spectrum of water is sensitive to temperature changes, so this will work also on other food products containing a large share of water.

To succeed with this type of measurement, the optical penetration depth is crucial. It is necessary to design the optical system so that the measured radiation has been deep enough into the product so that estimation of core temperature is possible. This puts a limitation on how thick the samples can be. If the samples are too thick, only the upper layer will be probed. If the temperature in this layer correlates well with the core temperature, it might be possible to estimate the core temperature.

This study shows that it is possible to estimate core temperature well also when different gradients are present. This requires more complex regression models that probably include information about typical spectral shape for different gradients, which again can be used to determine the core temperature. In most industrial heating processes, the temperature gradients in the products will be quite similar, since the

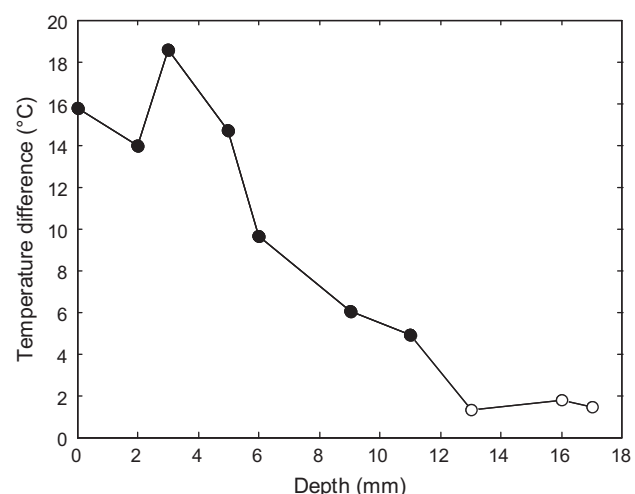


Fig. 6. Difference in estimated temperature between fish cakes without cold layer and with cold layer. Black markers indicate significant differences. White markers indicate non-significant differences.

heating process is much the same for all products. In such processes the regression models will probably be simpler and also more robust.

Of the two NIR systems that were evaluated, the point measurement system performed notably better than the imaging system. Both systems were based on interactance measurements, however, the point system did probably get better signals from deeper parts of the fish cake. For the point system, the light intensity at sample surface was higher and we used longer exposure time (1 s) on a small area/volume. The imaging system used 0.5 s to image the whole fish cake, meaning that more noisy signals could be expected. As seen in Fig. 3, we are modelling on rather small spectral shifts, and measurement accuracy is therefore crucial to obtain good calibration results for temperature.

To make robust calibrations it is probably wise to get an overview of variations in both core temperature and temperature gradients and include these in the calibration model. To prove that the NIR system of interest can actually probe deep enough to measure core temperature, an experiment like the one described in Section 2.4 could be conducted.

In this study we used an NIR spectrum that included three different water absorption peaks. The light around 980 nm is absorbed more strongly by water than at 760 and 840 nm. Hollis et al. (2001) suggested that the different wavelengths therefore will probe different depths in the material, 840 nm deeper than 980 nm. Since parts of the spectrum will be affected differently at different depths, the spectrum might contain information about possible gradients. Inclusion of all three absorption peaks in our study gave better results than modelling on only one or two. This is an interesting topic for further research.

Another interesting topic for this application is calibration transfer. We are mainly modelling on the shifts in the water absorbing bands as a function of temperature. Usually within NIR spectroscopy specific calibration models have to be made for different products, and so would the case be here. However, it would be of interest to investigate how a model designed for fish cakes would perform on for instance hamburgers, since the shifts according to temperature would probably be quite similar. The challenge would certainly be that hamburgers have different chemical composition and are also rich in myoglobin, which will result in different absorption and light scattering properties. However, it might be possible to simply use an offset and bias corrected regression model. The question of simplified calibration transfer would be of importance to suppliers of such systems, since it would reduce costs connected with installations in new process lines and for new products.

Although the imaging system obtained less accurate models in this work, the idea of imaging the whole conveyor and all passing products is good and fully possible. Such an imaging system can be optimised for the task by improving the optical design for maximum throughput of photons. Complete monitoring of the heat treated products could also be possible with a row of point sensors scanning different lanes on the conveyor. In this way the producer would have full control of the heating process and be sure that sufficient core temperature is reached in all product units. Such a system can also be used to control the temperature to a certain target that ensures safe products of high quality.

Acknowledgments

The research presented here was funded by the Norwegian Research Council through the project Novel Sensor technology and automation for improved quality and process control in the food industry (project number 199581/E40) and the Norwegian Agricultural Food Research Foundation through the project Food Imaging (project number 225347/F40). The financial support is greatly acknowledged. Martin Høy, Karen Wahlstrøm Sanden and Tom Johannessen are thanked for skilled technical assistance.

References

- Barnes, R. J., Dhanoa, M. S., & Lister, S. J. (1989). Standard normal variate transformation and de-trending of near-infrared diffuse reflectance spectra. *Applied Spectroscopy*, *43*, 772–777.
- Buning-Pfau, H. (2007). Analysis of water in food by near infrared spectroscopy. *Food Chemistry*, *82*, 107–115.
- Chen, T., & Martin, E. (2007). The impact of temperature variations on spectroscopic calibration modelling: A comparative study. *Journal of Chemometrics*, *21*, 198–207.
- Chung, S. H., Cerussi, A. E., Merritt, S. I., Ruth, J., & Tromberg, B. J. (2010). Non-invasive tissue temperature measurements based on quantitative diffuse optical spectroscopy (DOS) of water. *Physics in Medicine and Biology*, *55*, 3753–3765.
- ElMasry, G., & Wold, J. P. (2008). High-speed assessment of fat and water content distribution in fish fillets using online imaging spectroscopy. *Journal of Agricultural and Food Chemistry*, *56*, 7672–7677.
- Folkestad, A., Wold, J. P., Rorvik, K. A., Tschudi, J., Haugholdt, K. H., Kolstad, K., & Mørkøre, T. (2008). Rapid and non-invasive measurements of fat and pigment concentrations in live and slaughtered Atlantic salmon (*Salmo salar* L.). *Aquaculture*, *280*, 129–135.
- Gowen, A. A., Tiwari, B. K., Cullen, P. J., McDonnell, K., & O'Donnell, C. P. (2010). Applications of thermal imaging in food quality and safety assessment. *Trends in Food Science & Technology*, *21*, 190–200.
- Helgerud, T., Wold, J. P., Pedersen, J., Liland, K. H., Balance, S., Knutsen, S., ... Afseth, N. K. (2015). Towards on-line determination of dry matter content in whole unpeeled potato tubers using near-infrared spectroscopy. *Talanta*, *143*, 138–144.
- Hollis, V. S., Binzoni, T., & Delpy, D. T. (2001). Noninvasive monitoring of brain tissue temperature by near-infrared spectroscopy. *Proc. SPIE 4250, Optical Tomography and Spectroscopy of Tissue IV*, *470*–481.
- Ibarra, J. G., Tao, Y., & Xin, H. W. (2000). Combined IR imaging-neural network method for the estimation of internal temperature in cooked chicken meat. *Optical Engineering*, *39*, 3032–3038.
- Martens, H., & Næs, T. (1993). *Multivariate calibration*. New York: Wiley.
- O'Farrell, M., Wold, J. P., Høy, M., Tschudi, J., & Schulerud, H. (2010). On-line fat content classification of inhomogeneous pork trimmings using multispectral near infrared interactance imaging. *Journal of Near Infrared Spectroscopy*, *18*, 135–146.
- O'Farrell, M., Bakke, K. A. H., Tschudi, J., & Wold, J. P. (2011). Near-infrared (NIR) interactance system for non-contact monitoring of the temperature profile of baked liver pate. *Applied Spectroscopy*, *65*, 1372–1379.
- Ottestad, S., Høy, M., Stevik, A., & Wold, J. P. (2009). Prediction of ice fraction and fat content in superchilled salmon by non-contact interactance near infrared imaging. *Journal of Near Infrared Spectroscopy*, *17*, 77–87.
- Segtnan, V. H., Høy, M., Lundby, F., Narum, B., & Wold, J. P. (2009). Fat distributional analysis in salmon fillets using non-contact near infrared interactance imaging: A sampling and calibration strategy. *Journal of Near Infrared Spectroscopy*, *17*, 247–253.
- Wold, J. P., Johansen, I. R., Haugholdt, K. H., Tschudi, J., Thielemann, J. T., Segtnan, V. H., ... Wold, E. (2006). Non-contact transreflectance near infrared imaging for representative on-line sampling of dried salted coalfish (bacalao). *Journal of Near Infrared Spectroscopy*, *14*, 59–66.
- Wold, J. P., Kermitt, M., & Woll, A. (2010). Rapid nondestructive determination of edible meat content in crabs (*Cancer pagurus*) by near-infrared imaging spectroscopy. *Applied Spectroscopy*, *64*, 691–699.